

# **LIGHT SCATTERING MICROSCOPY FOR TUMOR CELL RECOGNITION**

Authors:

V. Richter, H. Schneckenburger

DOI: 10.12684/alt.1.59

Corresponding author: H. Schneckenburger

e-mail: herbert.schneckenburger@htw-aalen.de

---

# Light Scattering Microscopy for Tumor Cell Recognition

Verena Richter and Herbert Schneckenburger

Institut für Angewandte Forschung, Hochschule Aalen, Beethovenstr. 1, 73430 Aalen, Germany

## Abstract

Light scattering microscopy is suggested to provide some insight into cell architecture and to give information on cell malignancy or morphological changes upon necrosis or apoptosis. In the present paper a microscope setup for scattering experiments with high angular resolution is reported, and first data obtained from test models (polystyrene beads), cell monolayers and 3-dimensional cell spheroids are reported. Data are compared with simulations based on Mie scattering and discussed in view of their possible use for tumor cell recognition within tissue samples. The discussion includes present limitations due to spatial resolution or inhomogeneous illumination and suggests possibilities of improvement.

## Introduction

In label-free diagnostics of cells and tissues, intrinsic fluorescence and non-elastic light scattering appear to be promising methods. In particular, autofluorescence was used increasingly for tumor detection of various organs including bladder, lung, larynx, breast or skin [1–7]. When excited by near ultraviolet light, fluorescence of the coenzymes nicotinamid adenine dinucleotide (NADH) as well as flavin mono- and dinucleotide (FMN/FAD) seems to play a predominant role, since it reflects their state of oxidation and, consequently, cell physiology [8–10]. Previously, isogenic cell lines prior and subsequent to activation of tumor suppressor genes could be distinguished on the basis of their fluorescence spectra and decay times, and this difference was related to various metabolic pathways, in particular anaerobic glycolysis and respiration [11].

For a further distinction of tumor and less malignant cells, the application of Raman spectroscopy was suggested [12–14], and previous experiments of isogenic glioblastoma cells revealed slight differences in the vibrational spectra around  $970\text{ cm}^{-1}$  [15]. In the literature, also measurements of elastic scattering are reported, and angular dependence of light scattering [16] as well as wavelength dependent backscattering [17,18] were used to distinguish tumorigenic and non-tumorigenic cells or cells undergoing apoptosis. Measurements were based on differences in Mie

scattering by cells or organelles of various size and were commonly performed with cell suspensions or cells within a flow cytometer [19]. Since those measurements did not permit simultaneous visualization of sub-cellular structures, we now modified a conventional microscope for measuring elastic light scattering at high spatial and angular resolution.

## Materials and Methods

### *Samples*

#### *Test Models*

Polystyrene beads with a diameter of  $10.2\mu\text{m}$  were used to evaluate the setup. For measurements beads were suspended in sterile filtered Earl's Balanced Salt Solution (EBSS) and transferred to a glass capillary.

#### *Cell Cultures*

Chinese Hamster Ovary cells (CHO) were routinely grown in RPMI 1640 culture medium supplemented with 10% fetal calf serum (FCS) and 1% Penicillin/Streptomycin at  $37^\circ\text{C}$  and 5%  $\text{CO}_2$ . MCF-7 human breast carcinoma cells were cultivated in DMEM/Ham's F-12 culture medium supplemented with 10% fetal calf serum (FCS) and 1% Penicillin/Streptomycin at  $37^\circ\text{C}$  and 5%  $\text{CO}_2$ . For measurement of single cells or small cell clusters, CHO cells were cultivated as monolayers on glass slides.

#### *Cell Spheroids*

After seeding 200 cells per well in a 96 well plate coated with agarose to prevent the cells from adhesion at the bottom, multi-cellular spheroids of MCF-7 breast cancer cells were cultivated for one week in DMEM/Ham's F-12 culture medium supplemented with 10% fetal calf serum (FCS) and 1% Penicillin/Streptomycin at  $37^\circ\text{C}$  and 5%  $\text{CO}_2$ . For measurements spheroids were transferred to a glass capillary of rectangular shape with the dimensions  $4.25 \times 1.25 \times 50\text{mm}$  (Hilgenberg GmbH, Malsfeld, Germany). All probes were measured in sterile filtered EBSS or Hepes to reduce the scattering background.

## Microscopy

For measurement of light scattering cell monolayers or cell spheroids located either on a cover slide or within a micro-capillary were illuminated within an inverted microscope (Axiovert 200, Carl Zeiss Jena, Germany). The expanded beam of a 470 nm laser diode (LDH 470 with driver PDL 800-B, PicoQuant, Berlin, Germany) was deflected by an adjustable mirror and focused into the aperture of the microscope objective lens (40x/0.75 or 40x/1.30 oil immersion) as described earlier [20]. Thus, the samples were illuminated by a parallel beam under variable angles. Scattered light was collected by the same objective lens, selected by a beam splitter and further focused by a Bertrand lens generating an image of the aperture plane. Within this image a central region of  $\pm 1^\circ$  was selected by a tiny aperture, so that backscattering could be measured in an angular range between slightly above  $180^\circ$  and  $225\text{--}240^\circ$ . A scheme of the setup is depicted in Figure 1. Measurements were combined with microscopic imaging of the aperture plane (using the Bertrand lens) or the object plane (omitting the Bertrand lens).

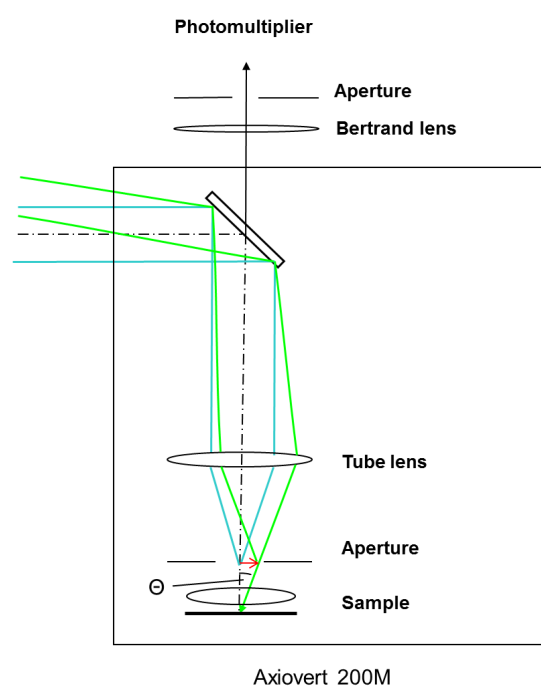


Figure 1  
Microscope setup for backscattering experiments with angular resolution.

## Results

### Simulation

Figure 2 shows the simulated phase function for Mie scattering (non-polarized light) by single polystyrene beads with diameters of  $4\mu\text{m}$ ,  $8\mu\text{m}$  and  $16\mu\text{m}$ , assuming refractive indices of  $n_b = 1.59$  for the beads and  $n_m = 1.334$  for the surrounding

medium (EBSS). All phase functions exhibit pronounced minima, whose frequency increases with increasing diameter of the scatterers. Phase functions were sensitive even to small changes of the size (around  $20\text{nm}$ ) or the refractive index (around  $0.01$ ) of the beads.

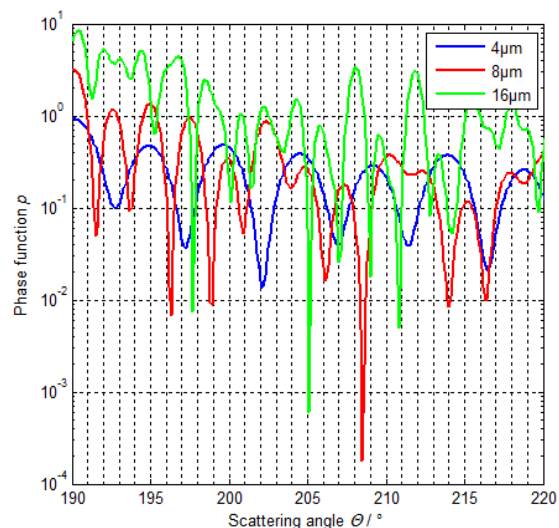


Figure 2

Simulated phase function for single polystyrene beads with diameters of  $4\mu\text{m}$ ,  $8\mu\text{m}$  and  $16\mu\text{m}$  assuming refractive indices of  $n_b = 1.59$  (bead) and  $n_m = 1.334$  (surrounding medium).

### Bead Measurements

To compare simulations and experiments of light scattering with angular resolution, we used polystyrene beads of various diameters. Some agreement was found for beads of various sizes, e.g.  $10.2 \pm 0.02 \mu\text{m}$  in comparison with theoretical spheres of  $10.2 \mu\text{m}$  diameter and a refractive index of  $1.59$ , as depicted in Figure 3.

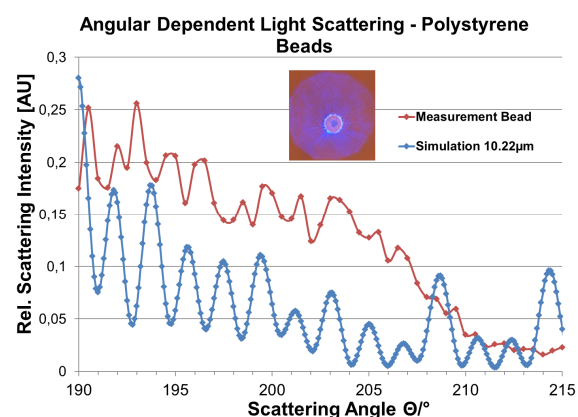


Figure 3

Angular dependence of light scattering of polystyrene beads in the range of  $190^\circ\text{--}220^\circ$ ;

red line: measurement of a bead with  $\varnothing 10.2 \pm 0.02 \mu\text{m}$ ;  
blue line: simulation for a sphere with  $\varnothing 10.22 \mu\text{m}$   
(excitation wavelength:  $470 \pm 5 \text{ nm}$ ; Plan-Neofluar 40x/1.30 microscope objective lens with immersion oil).  
Inlay: image of the object plane with scattering beads.

## Cell Measurements

First results of angular dependent light scattering of living cells were obtained from CHO colonies on glass slides. Figure 4 shows measurements of a healthy colony (red line) in comparison with a colony in an advanced state of decline, exhibiting numerous blebs and increasing amounts of cell fragments (blue line). These degraded cells are characterized by an angular dependence of light scattering which is similar to the phase function of small spheres (with repeated scattering minima every 4–5 degrees, cf. Figure 1). Less pronounced minima appearing at a higher frequency are observed for the healthy cells, since in this case scattering is expected to originate mainly from the comparably large (whole) cells.

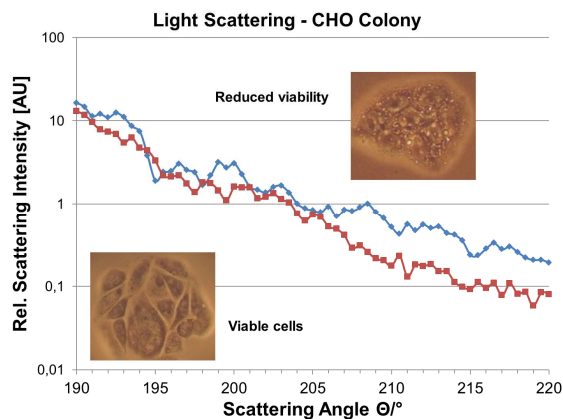


Figure 4  
Angular dependence of light scattering of CHO cells in the range of 190°–220°;  
red line: healthy colony; blue line: degraded colony with blebs and cell fragments (excitation wavelength: 470±5 nm; Plan-Neofluar 40x/0.75 microscope objective lens);  
Inlay: transmission microscopy of both colonies.

## Spheroid Measurements

In a first step towards tumor detection by measurements of angular dependent light scattering we analyzed spheroids of MCF-7 breast cancer cells with an average diameter of 200 μm. By an appropriate aperture the field of view could be varied between about 30 μm and 250 μm to select an area of interest. In addition, focal planes with different distances  $z$  from the bottom of the spheroid could be imaged. Typical results are depicted in Figure 5, with the focal plane being located at  $z = 0$  μm (red curve) or  $z = 60$  μm (blue curve). Cellular structures are more evident in the second case and may result in more pronounced maxima and minima in the angular dependence of light scattering (Figure 5).

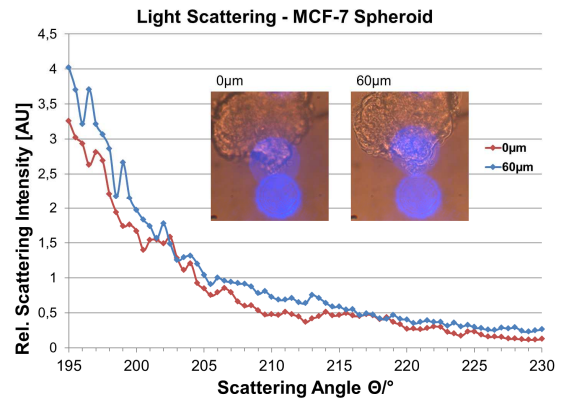


Figure 5  
Angular dependence of light scattering of a MCF-7 spheroid with a focal plane at 0 μm (red line) or 60 μm (blue line) from the glass slide; angular range 195°–230°; illuminated field ~90 μm, as marked by the upper blue light spot (the lower spot corresponds to an artifact)  
(excitation wavelength: 470±5 nm; Plan-Neofluar 40x/1.3 microscope objective lens with oil immersion).

## Discussion

According to our preliminary results (and also to those of other authors) elastic light scattering may offer some information on cell morphology, which is complementary to parameters describing cell function, e.g. autofluorescence or Raman scattering. The advantage of our present setup is that small object fields can be selected in the microscope permitting measurements even of single cells or small tissue (e.g. tumor) sections of specific interest. Object size can be limited by appropriate diaphragms in the microscope (in our case about 30 μm). However, the light spot on the sample is not diffraction limited, since the laser is focused into the aperture plane of the microscope, resulting in a parallel beam in the plane of the sample.

A further question is related to the optimum coherence length of laser light, which should be larger than the scattering objects to profit from interference patterns occurring in Mie scattering. On the other hand, additional interference may arise from various parts within the microscope, and artefacts may be created, if the coherence length is too long. In the present case a coherence length of the laser diode of 220 μm (determined by a Michelson interferometer) appeared to be appropriate to resolve Mie scattering and to avoid most artefacts. However, some inhomogeneous illumination of the samples could not be totally excluded.

Light scattering by several cells and sub-cellular structures may result in rather complex interference patterns, and angular resolution in two rather than in one direction might give additional information about individual scatterers. Therefore, rotation of the samples is planned in future experiments. In addition, measurements with polarized light [21,22]

could provide further information on sub-cellular architecture.

Since Mie scattering is very sensitive to the refractive indices of the scatterers and the surrounding medium, it appears difficult to determine sizes of the scattering particles in absolute units. However, it appears possible to measure differences between tumor cells and less malignant cells, if these cells have different morphologies, e.g. different sizes of their nuclei. It appears also possible to measure swelling or shrinking processes upon necrosis or apoptosis. Only future experiments may prove, whether mixed cultures of tumor and less malignant cells can be analyzed or whether cancer cells infiltrating healthy tissue can be detected by light scattering experiments.

### Acknowledgment

We would like to thank Baden-Württemberg-Stiftung gGmbH for financing project "Mistral". We also thank Prof. Alwin Kienle, Dr. Michael Schmitz and Thomas Rothe (ILM Ulm) for providing the simulation software as well as for stimulating discussions. Critical reading of this manuscript by Dr. Petra Weber and skillful technical assistance by Claudia Hintze are gratefully acknowledged.

### References

- [1] S. Andersson-Engels, J. Johansson, K. Svanberg, K., and S. Svanberg, (1991) Fluorescence imaging and point measurements of tissue: applications to the demarcation of malignant tumors and atherosclerotic lesions from normal tissue, *Photochem. Photobiol.* 53 (6), 807-814.
- [2] J. Hung, S. Lam, J.C. LeRiche, and B. Palcic (1991) Autofluorescence of normal and malignant bronchial tissue, *Lasers Surg. Med.* 11 (2), 99-105.
- [3] B. Banerjee, B. Miedema, and H.R. Chandrasekhar (1998) Emission spectra of colonic tissue and endogenous fluorophores", *Am. J. Med. Sci.* 316 (3), 220-226.
- [4] M.A. d'Hallewin, L. Bezdetnaya, and F. Guillemin (2002) Fluorescence detection of bladder cancer: a review, *Eur Urol.* 42(5), 417-425.
- [5] D.C. de Veld, M.J. Witjes, H.J. Sterenberg, and J.L. Roodenburg (2005) The status of in vivo autofluorescence spectroscopy and imaging for oral oncology, *Oral Oncol.* 41(2), 117-131.
- [6] M. Monici (2005) Cell and tissue autofluorescence research and diagnostic applications, *Biotechnol. Annu. Rev.* 11, 227-256.
- [7] T. Gabrecht, Glanzmann, L. Freitag, B.C. Weber, H. van den Bergh, and G. Wagnières (2007) Optimized autofluorescence bronchoscopy using additional backscattered red light, *J. Biomed. Opt.* 12(6), 064016.
- [8] T. Galeotti, G.D.V. van Rossum, D.H. Mayer, and B. Chance (1970) On the fluorescence of NAD(P)H in whole cell preparations of tumors and normal tissues, *Eur. J. Biochem.* 17, 485-496.
- [9] J.-M. Salmon, E. Kohen, P. Viallet, J.G. Hirschberg, A.W. Wouters, C. Kohen, and B. Thorell (1982) Microspectrofluorometric approach to the study of free/bound NAD(P)H ratio as metabolic indicator in various cell types, *Photochem. Photobiol.* 36, 585-593.
- [10] A.A. Heikal (2010) Intracellular coenzymes as natural biomarkers for metabolic activities and mitochondrial anomalies, *Biomark. Med.* 4(2), 241-263.
- [11] P. Weber, M. Wagner, P. Kioschis, W. Kessler, and H. Schneckenburger (2012) Tumor cell differentiation by label-free fluorescence microscopy, *J. Biomed. Opt.* 17(10), 101508.
- [12] I.F. Nabiev, H. Morjani, and M. Manfait (1991) Selective analysis of antitumor drug interaction with living cells as probed by surface-enhanced Raman spectroscopy, *Eur. Biophys. J.* 19(6), 311-316.
- [13] K. Chen, Y. Qin, F. Zheng, M. Sun, and D. Shi (2006) Diagnosis of colorectal cancer using Raman spectroscopy of laser-trapped single living epithelial cells, *Opt. Lett.* 31(13), 2015-2017.
- [14] C.M. Krishna, J. Kurien, S. Mathew, L. Rao, K. Madheedkar, K.K. Kumar, and M.V. Chowdary (2008) Raman spectroscopy of breast tissues, *Expert Rev. Mol. Diagn.* 8 (2), 149-166.
- [15] H. Schneckenburger, P. Weber, M. Wagner, M. Brantsch, Ph. Biller, P. Kioschis, and W. Kessler (2011) Tumor cell differentiation by marker free fluorescence microscopy, in *Proc. SPIE*, 7902, 79020D.
- [16] J.R. Mourant, T.M. Johnson, V. Doddi, and J.P. Freyer (2002) Angular dependent light scattering from multicellular spheroids, *J. Biomed. Opt.* 7(1), 93-99.
- [17] M. Xu, T.T. Wu, and J.Y. Qu (2008) Unified Mie and fractal scattering by cells and experimental study on application in optical characterization of cellular and subcellular structures, *J. Biomed. Opt.* 13(2), 024015.
- [18] Ch. Mulvey, C.A. Sherwood, and I.J. Bigio (2009) Wavelength-dependent backscattering

measurements for quantitative real-time monitoring of apoptosis in living cells, *J. Biomed.Opt.* 14(6), 064013.

[19] Y.-L. Pan, M.J. Berg, S. Sm. Zhang, H. Noh, H. Cao, R.K. Chang, and G. Videen (2011) Measurement and autocorrelation analysis of two-dimensional light-scattering patterns from living cells for label-free classification, *Cytometry* 79A, 284-292.

[20] H. Schneckenburger, H. Baumann, M. Wagner, and W.S.L. Strauss (2007) Axially Resolved Cell Imaging by Intensity Modulated Total Internal Reflection Fluorescence Microscopy (IM-TIRFM), in *Proc. SPIE* 6441, 64411E.

[21] J. R. Mourant, T. M. Johnson, S. Carpenter, A. Guerra, T. Aida, and J. P. Freyer (2002) Polarized angular dependent spectroscopy of epithelial cells and epithelial cell nuclei to determine the size scale of scattering structures, *J. Biomed. Opt.* 7(3), 378-387.

[22] F. Voit , A. Hohmann, J. Schäfer, and A. Kienle, (2012) Multiple scattering of polarized light: comparison of Maxwell theory and radiative transfer theory, *J. Biomed. Opt.* 17(4), 045003.